X-ray Absorption Study of Copper(II)−Glycinate Complexes in Aqueous Solution

P. D'Angelo,*,† E. Bottari,† M. R. Festa,† H.-F. Nolting,‡ and N. V. Pavel*,†

Dipartimento di Chimica, Università degli Studi di Roma "La Sapienza", Piazzale Aldo Moro 5, I-00185, Roma, Italy, and EMBL Outstation Hamburg, c/o DESY, Notkestrasse 85, D-22603, Hamburg, Germany

Received: October 28, 1997; In Final Form: February 9, 1998

The structures of the mono-, bis-, and tris(glycinato)copper(II) complexes in aqueous solution have been determined by X-ray absorption spectroscopy. Four solutions with different complex ratios have been examined, and the species concentrations have been determined on the basis of complex stability constants. An advanced data analysis including multiple-scattering effects and multielectron excitation processes produced quantitative information on the Cu(II)−glycinate complexes present in aqueous solution. The structure of the bis(glycinato)copper(II) complex, which has a low solubility in water, has been determined for the first time. It has been found to have a distorted octahedral geometry with two bidentate glycine ligands coordinating to the Cu^{2+} ion in the equatorial plane and with the axial sites occupied by two additional water molecules at 2.40 ± 0.06 Å. Analysis of the X-ray absorption data allowed a detailed description of the structures of the mono- and tris(glycinato)copper(II) species. The former complex has an axially elongated octahedral structure with a glycine bidentate ligand and two water molecules placed at the equatorial and two water molecules at the axial positions (2.44 ± 0.08 Å). Experimental data for the latter complex were also explained in terms of a distorted octahedral model with two glycine molecules in the equatorial plane and with the amino nitrogen of the third glycine coordinating to the Cu^{2+} ion at the axial site at a distance of 2.33 ± 0.05 Å. This result conflicts with the regular octahedral geometry previously determined by XRD investigations. The axial bonds of the three complexes are significatively longer than the average within the hexaaquocopper-(II) ions**.** This finding indicates that the axial bonds are lengthened upon the formation of the Cu−glycine complexes and the Cu(II)−water interaction at the axial site is weakened.

Introduction[1]

Transition metals such as iron, cobalt, copper, zinc, and manganese play an important role in biological processes,[2,3] whereas lead, cadmium, and mercury are toxic for many living systems.[4,5] The essential metals are present in many biological fluids as free ions or complexed by metalloproteins and low-molecular mass substances including peptides and amino acids. Metal-binding proteins are relatively easy to isolate and many of them are well characterized. In contrast, low-molecular-weight complexes are part of multicomponent systems with different complexing species in equilibrium. Knowledge of the structure and equilibrium distribution of metal ion−amino acid complexes present in aqueous solutions can be useful in explaining many biological processes.

A description of different species existing in water solution, as well as their relevant ratios, is provided by complex stability constants. Most of these constants have been reported in the literature[6−8] together with critical analyses of the experimental methods employed in their investigation.[9−11] In the case of amino acids, electromotive-force measurements provide the highest precision and accuracy.[11] The constant ionic medium method proposed by Biedermann and Sillén[12] is frequently used to minimize variations of the activity coefficients due to the change in the reagent concentrations. This allows activities to be replaced by concentrations.

Mixed amino acid peptide Cu(II) complexes in aqueous solution have received considerable attention because of their involvement in the transport of Cu(II) ions in biological systems.[2,13−15] Significant results have been obtained by Olin et al.[16] on the Cu(II)−aspartate, −valine, and −proline aqueous solution systems. Olin has proposed that Cu(II)−amino acid complexes in aqueous solutions are five-membered chelates with the amino and carboxylate groups binding to the copper ion. The conclusions of these studies are mainly based on stability constants calculated from the complex formation function. This function has been determined by measuring the free hydrogen ion concentration (c_h) of solutions containing the cation and amino acids (typically in the ratio 1:1, 1:2, or 1:3) with a glass electrode in titrations with a strong base.

Complex formation between Cu(II), Zn(II), Cd(II), Pb(II), Fe(II), Fe(III) and glycine, serine, α- and β-alanine, aspartate, glutamate, histidine, and ornithine has been investigated by measuring the emf of galvanic cells with a glass and an amalgam or redox electrode of the studied metal in a wide range of concentrations of the reagents.[17,18] Experimental data have been explained by assuming the presence of different species and deriving the respective stability constants.

Electromotive-force measurements allow the identification of the prevailing complexes and their stability constants, but they give no structural information on the metal coordination of the species found in solution. The models proposed in the emf studies are based on structural information obtained from single-crystal X-ray diffraction analysis of a large number of metal−amino acid complexes.[19,20] However, complexes that can be

* To whom correspondence should be addressed.
† Università degli Studi di Roma "La Sapienza".
‡ EMBL Outstation Hamburg.

S1089-5647(97)03476-7 CCC: $15.00
Published on Web 04/02/1998

crystallized represent a minor percentage of the species present in dilute solutions of physiological relevance.

Previous investigations of the structures of Ni(II)−,[21] Cu(II)−,[22] and Zn(II)−glycinate[23] complexes in aqueous solutions have been performed by means of X-ray diffraction. This technique is not applicable to dilute systems, and for this reason solutions containing high concentrations of metal ions (from 0.7 to 3.0 M), which are not present in biological fluids, have been investigated. Possible structures of mono- and tris(glycinato) complexes have been proposed, whereas the structures of the bis(glycinato) complexes, which have low solubility in water, have not been determined.

X-ray absorption spectroscopy is more suitable than X-ray and neutron diffraction for the investigation of metal−amino acid interactions in dilute solutions. This is due to the fact that the partial distribution functions around a single atom type (the photoabsorber atom) can be determined and experiments can be performed at low metal concentrations. Use of the XAS technique in fluorescence mode allows structural information to be obtained at a metal concentration in the range from 1 to 5 mM. The structures of bis- and tris(glycinato) complexes of Ni(II) and Zn(II) ions in aqueous solutions have been investigated by extended X-ray absorption fine-structure measurements in transmission mode.[24] Nevertheless, the low solubility of the bis(glycinato)Cu(II) complex in water (∼25 mM) hampered the determination of the structure of this complex.[24] Successively, Ozutsumi et al.[25] have performed an EXAFS study of several mono- and bis(amino acidato)copper(II) complexes in solution at high Cu(II) concentrations. In the case of the Cu(II)−glycinato complexes only the structural parameters of the mono(glycinato)Cu(II) species have been determined.

In this paper a thorough structural investigation of Cu(II)−glycine complexes present in aqueous solutions has been carried out. Use of the EXAFS technique in fluorescence mode allowed the investigation of dilute Cu(II) solutions (5 mM). Previous studies of the species and their respective ratios in solutions have been performed by Bottari et al.[17] in a wide c_h range.

Experimental Section

Cu(II)−Glycinate Complexes Investigated. The composition of the investigated solutions was selected on the basis of the results previously obtained for the Cu(II)−glycine system[17] and for the protonation of glycine in aqueous solutions.[26] Electromotive-force data were obtained by using glass and copper amalgam electrodes in a wide range of concentrations of the reagents. The results were explained by assuming the presence of four complexes, namely, CuL ($\log \beta_{1,0,1} = 8.39 \pm 0.05$), CuHL ($\log \beta_{1,1,1} = 10.62 \pm 0.10$), CuL_2 ($\log \beta_{1,0,2} = 15.32 \pm 0.04$), and CuL_3 ($\log \beta_{1,0,3} = 16.96 \pm 0.08$).[27]

Four samples have been prepared in order to maximize the concentration of the complexes under investigation, namely, CuL_2 (samples 1 and 2), CuL (sample 3), and CuL_3 (sample 4).

Inspection of the $\log \beta$ values shows that the CuL_2 species prevails in a large range of concentrations of the reagents while the other complexes are present in very small amounts (less than 1%). From the distribution curves of the species as a function of $\log c_h$ at $C_L = 0.100$ M, it appears that the CuL_2 complex prevails in the range $6 \leq -\log c_h \leq 8$. In the above range the CuL_2 complex has a percentage higher than 99%, whereas CuL is present at 0.3% and CuL_3 at about 0.6%. From previous investigations the presence of hydrolytic species of copper in these solutions can be discarded.[17,28,29]

Sample 1, 99.1 ± 0.2% in CuL_2, had the following composition: $C_{Cu} = 5$ mM, $C_L = 0.100 + 2C_{Cu} = 0.110$ M, $C_{Na^+} = (1 - 2C_{Cu} - C_H)$ M, and $C_{ClO_4^-} = 1$ M. The $-\log c_h$ of the solution was adjusted at 7.0 by adding the required amount of NaOH.

Sample 2 had the same composition as sample 1, and its $-\log c_h$ was adjusted at 4 by adding the required amount of $HClO_4$. In this case the prevailing species are CuL_2 (60 ± 5%) and CuL (40 ± 5%), while CuHL and Cu^{2+} are present at values less than 1% and CuL_3 is practically absent. The CuL_2 and CuL concentration values have a correlation coefficient equal to −1.

Solutions with higher percentages of CuHL or CuL_3 can be obtained by increasing the total concentration of glycine to 0.5 M. However, under these conditions of Cu(II) and glycine concentrations, the maximum concentration of CuHL cannot exceed 10%. Sample 3 has been prepared at $-\log c_h = 3$ in the same ionic medium, with the same C_{Cu} (5 mM) and C_L (0.500 M) values. The species present in solution are CuHL (9.3 ± 1.0%), CuL (54.6 ± 0.1%), CuL_2 (33.0 ± 0.8%), and Cu^{2+} (3.1 ± 0.4%).

High CuL_3 concentration can be obtained by increasing the $-\log c_h$. Sample 4 has the same composition as sample 3 and a $-\log c_h$ value of 10. This solution contains 93.4 ± 1.5% of CuL_3 and 6.6 ± 1.5% of CuL_2.

EXAFS Data Collection and Analysis. X-ray absorption spectra at the Cu K edge were recorded in fluorescence mode using the EMBL spectrometer[30] at HASYLAB and synchrotron radiation from the storage ring DORIS III (4.5 GeV and positron currents between 70 and 40 mA). Measurements were performed at room temperature using a Si(111) double-crystal monochromator and a focusing toroidal mirror. Selected Bragg reflections of a suitably mounted Si crystal simultaneously recorded with the spectrum were used for the absolute energy calibration.[31] The spectra were recorded in the range 8725−9710 eV using a 13-element Ge detector (Canberra). A check was performed by collecting the data for a 5 mM $Cu(ClO_4)_2$ solution. The EXAFS data analysis of this sample was consistent with the results previously obtained for a $Cu(ClO_4)_2$ water solution measured in transmission mode.[32] The solutions were kept in cells with a Teflon spacer (2 mm) and Kapton film windows. From the width of the peaks of the calibrator, the energy resolution of the monochromator could be determined experimentally as 2.0 eV.

Data Evaluation. A quantitative analysis of the EXAFS data has been performed using the GNXAS set of programs. For a detailed description of this method see refs 33 and 34. The first step of the analysis involves the ab initio calculation of the X-ray absorption cross section of the systems under consideration, using the multiple-scattering theory. The theoretical structural signal $\chi(k)$ is calculated as a sum of the two-body (SS) and three-body MS signals $\gamma_j^n(k)$ associated with the n-atom configurations including the photoabsorber. The two-body signals are associated with pairs of atoms and probe their distances and variances. The three-body signals are associated with triplets of atoms and probe angles and their variances.

In the standard EXAFS analysis, the coordination of the photoabsorber is usually described by Gaussian shells, taking into account small disorder within the harmonic approximation. In the case of solutions, the radial distribution functions associated with the solvent molecules are asymmetric and the Gaussian approximation is totally inadequate. A method that employs Γ-like distribution curves to reproduce the asymmetry in the distribution functions has been recently applied to the

EXAFS analysis of ions and small molecules in solution.[32,35−40] According to this method each asymmetric peak is defined by the mean distance R, the distance mean-square variance σ^2, the skewness β, and the coordination number N. Owing to the asymmetry, the mean distance R does not coincide with the modal value of the distribution. Previous studies have shown that for disordered systems the accuracy of the EXAFS data analysis is significantly improved by using asymmetric shells. A comparison of the results obtained from Gaussian and asymmetric peaks has recently been accomplished.[39]

Phase shifts for the photoabsorber and backscatterer atoms have been calculated on the basis of the bis(glycinato)copper-(II) monohydrate crystal structure[41] by using muffin-tin potentials and advanced models for the energy-dependent exchange-correlation self-energy (Hedin-Lundqvist).[42] The muffin-tin radii have been chosen to be in agreement with standard prescriptions. They were 1.04, 0.75, 0.83, and 0.70 Å for copper, oxygen, nitrogen, and carbon atoms, respectively. Data analysis has been carried out by using a fitting procedure applied to the raw fluorescence data. The presence of anomalous features associated with the 1s3p double-electron excitation has recently been observed in the absorption spectra of cupric compounds above the K edge.[43] Here, the background functions used to extract the $\chi(k)$ experimental signals have been modeled by means of step-shaped functions in order to account for double-electron resonances. In all the samples under investigation the double-excitation channel has been found at 85 ± 5 eV above the K edge with a step height about 3−4% of the K-edge jump, in agreement with previous determinations.[32,43]

During the fitting procedure six nonstructural parameters have been varied: E_0, which allows the theoretical and experimental k scales to be compared; S_0^2, which accounts for the reduced overlap between the passive electrons in the ground state and in the excited-state relaxed configurations; δ, which represents the experimental resolution and the three parameters describing the double-excitation edge. The mean values obtained for E_0, S_0^2, and δ are 8990.0 ± 0.3 eV, 0.96 ± 0.02, and 2.9 ± 0.1 eV, respectively. The quality of the fits has been determined by the goodness-of-fit parameters[34] and by inspection of the EXAFS residuals and FTs. The number of variables employed in the data analyses is 27 for sample 1 and is 29 for samples 2−4. A rough estimate of the free parameters that can be fitted is given by the $2\Delta k\Delta R/\pi + 2$ rule,[44] which supports the present least-squares fitting procedure. Δk is the k-space range over which the $\chi(k)$ signal is fitted, and ΔR is the width of the R-space Fourier filter window. In our case, Δk is about 12 Å^{-1} and ΔR is limited by the mean-free path only, since we are not Fourier filtering the data.

Results and Discussion

Near-Edge Structure. The edge regions of the normalized fluorescence spectra and their derivatives are shown in Figure 1. The edge spectra are compared with a 5 mM $Cu(ClO_4)_2$ solution spectrum. They exhibit a very low preedge peak at 8979 eV and a shoulder on the rising edge defined as the first inflection point of the spectra at approximately 8986 eV. These features have been detected in the absorption spectra of other Cu(II) complexes and have been assigned to a 1s → 3d transition[45] and to a 1s → 4p + ligand−metal charge-transfer shakedown transition,[46,47] respectively. The positions and the intensities of these features are typical of Cu(II) with a 6-fold (4 + 2) coordination by N/O donors.[46b,48,49] The latter transition is broadened when Cu(II) binds a smaller amount of ligand (sample 3), and it disappears in the case of hexaaquocopper(II)

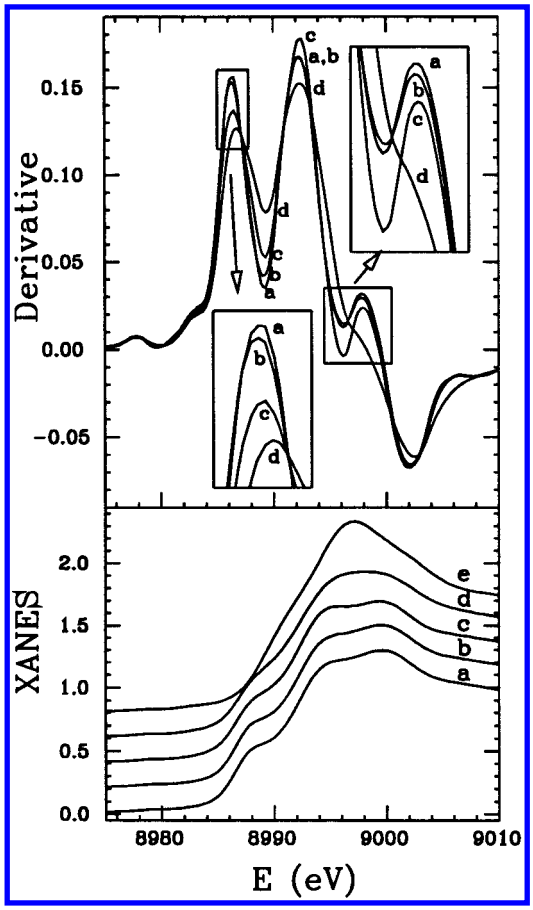

Figure 1. Cu K edge region of the normalized fluorescence spectra (bottom) and their derivatives (top): (a) sample 1, (b) sample 2, (c) sample 3, (d) sample 4. The edge spectra are compared with a 5 mM $Cu(ClO_4)_2$ solution spectrum (e).

complexes. The absorption edge of the CuL_3 complex shows two broad principal maxima located around 8996 and 9000 eV, respectively. The former feature becomes prominent for samples 1 and 2, whereas sample 3 presents a featureless edge, similar to $Cu(ClO_4)_2$.

Structure of the Bis(glycinato)copper(II) Complex. To gain a thorough understanding of the structural organization of the CuL_2 complex in aqueous solutions, a careful EXAFS analysis of sample 1 has been carried out. The crystallization conditions of both the cis and trans isomers of bis(glycinato)-copper(II) monohydrate are described in the literature,[50] but only the crystal structure of the cis isomer is known.[41] Two glycine molecules are chelated to the Cu(II) ion, giving rise to an approximately planar cis configuration with a low degree of "puckering" of the chelate rings. Each $C_\alpha-CO-O$ group is nearly planar, and the corresponding amino nitrogen atom slightly deviates from the plane. The four ligand atoms are not strictly coplanar and the Cu(II) ion lies 0.05 Å out of their least-squares plane, giving rise to two N−Cu−O angles of 175° and 178°. One water molecule (Cu−O = 2.405 Å) and an adjacent carboxyl oxygen (Cu−O = 2.74 Å) complete the distorted octahedral coordination of the Cu(II) ion.

The cis Cu(II)−glycinate crystal geometry has been chosen as the structural model for the EXAFS data analysis. Two water molecules (O_{ax}) have been placed in the axial positions, as shown in Figure 2, and their distances have been determined from the EXAFS minimization. The experimental spectrum contains also a high-frequency contribution, which is associated with the second hydration shell ($Cu-O_s$) as previously found in the EXAFS spectra of dilute Cu^{2+} aqueous solution.[32,36]

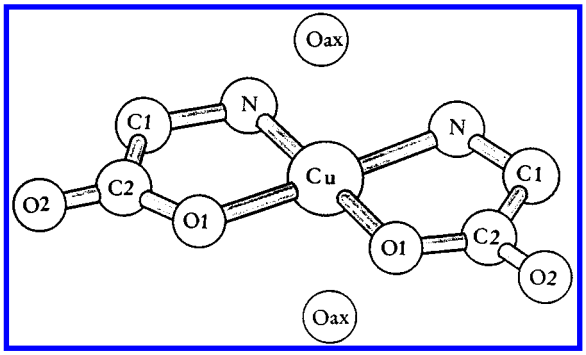

Figure 2. Geometry of the *cis*-bis(glycinato)copper(II) dihydrate complex in aqueous solution.

Asymmetric peaks have been used to describe the Cu−O_{ax} and Cu−O_s contributions as outlined in the previous section.

SS and MS signals have been calculated for all the two-body and three-body configurations associated with two glycine molecules chelated to the Cu(II) ion. Owing to the focusing effect, the amplitude of the three-body signals associated with quasi-linear configurations is strongly enhanced. For this reason the MS contributions associated with "nonlinear" configurations (with angles smaller than 160°) are of negligible amplitude and have not been included in the theoretical signal. On the other hand, the two Cu−C2−O2 and the two quasi-linear N−Cu−O1 configurations produce strong MS contributions that have been accounted for in the EXAFS data analysis. Note that the former signal is present only if the glycinate ion acts as a bidentate chelate. If the amino acid was coordinated to the copper atom through the carboxy oxygen or the amino nitrogen atom only, the conformational freedom would not have allowed a rigid Cu−C2−O2 configuration to form and no MS signal would have been detected.

It is worth stressing that the cis isomer cannot be assumed a priori as the only species present in our sample. The most important stereochemical difference between the cis and trans configurations, from the EXAFS data analysis point of view, is associated with the quasi-linear three-body configurations in the equatorial plane. The EXAFS technique could discriminate between the cis and the trans CuL_2 configuration only on the basis of the difference between two N−Cu−O1 (cis configuration) and one O1−Cu−O1 plus one N−Cu−N (trans configuration) three-body contributions. Since the backscattering amplitudes and phases of nitrogen and oxygen atoms are very similar, these signals are practically equal. Therefore, the calculated total signals of the two isomers are equivalent and the EXAFS technique cannot distinguish one isomer from the other.

Least-squares fits of all the experimental spectra have been performed in the range $k = 2.5-14.6$ Å^{-1}. The Cu−ligand signals have been calculated using fixed coordination numbers and variable Debye−Waller factors. During the minimization, the shell distances and angles have been varied within a narrow range (0.05 Å and 8°, respectively) around the mean crystallographic values. The Cu−O_{ax} and Cu−O_s shell parameters of the hexaaquocopper(II) complex[37] have been used as starting values and have been varied during the refinement in order to obtain the best agreement between experimental and theoretical signals. The Cu−O_{ax} coordination number has been fixed at 2. Figure 3a shows the best-fit analysis of the EXAFS spectrum of sample 1. The first curve from the top includes all the SS signals associated with the two glycine molecules complexed to the Cu(II) ion. The second and third curves in Figure 3a are the three-body signals associated with the in-plane quasi-linear

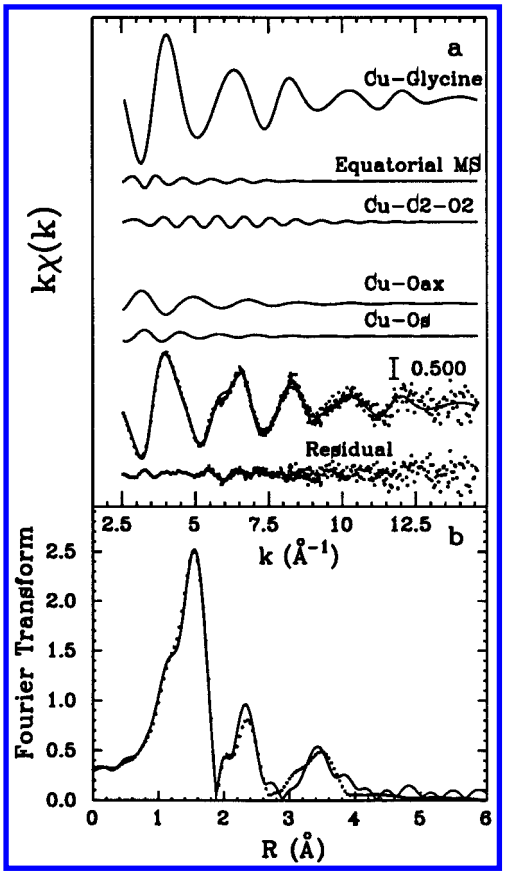

Figure 3. Comparison of the theoretical (−) and experimental (···) signals of the *k*-weighted EXAFS data and FT of sample 1: (a) from top to bottom, total Cu−glycine SS, equatorial MS, Cu−C2−O2, Cu−O_{ax}, and Cu−O_s calculated signals, their sum compared with the experimental spectrum, and the residual; (b) nonphase-shift-corrected FT of the experimental data and of the total theoretical signal.

N−Cu−O1 and with the Cu−C2−O2 configurations, respectively. The two additional curves represent the Cu−O_{ax} signal and the second hydration-shell contributions. The remainder of the figure shows the total theoretical contribution compared with the experimental spectrum and the resulting residual. The Fourier transform moduli of the experimental and theoretical spectra are shown in Figure 3b. Overall, the fitted EXAFS spectrum and its FT match the experimental data quite well and the high-*k* behavior of the residual curve reflects the noise of the experimental spectrum. Note that the signal-to-noise ratio of fluorescence data is usually 1 order of magnitude smaller than in the case of transmission data. From Figure 3a it is evident that the total $\chi(k)$ signal is dominated by the first-shell contributions. Nevertheless, the inclusion of the additional signals is essential to properly reproduce the high-frequency pattern of the experimental spectrum. The first two peaks in the FT at ∼1.6 and 2.4 Å are well accounted for by the Cu−glycine and Cu−O_{ax} signals. The three-body N−Cu−O1 and Cu−C2−O2 contributions are relatively strong, and together with the second hydration-shell signal, they account for the nonphase-shift-corrected FT peak at ∼3.5 Å.

The structural parameters as derived from EXAFS data analysis are reported in Table 1, together with crystallographic distances and angles. Statistical errors are given for the structural parameters that have been determined exclusively from the EXAFS analysis. They have been estimated by looking at the confidence interval in the parameter's space. Standard deviation and correlation effects have been obtained from the correlation maps determined for each couple of parameters. The

TABLE 1: Crystallographic Values of *cis*-Bis(glycinato)copper(II) Monohydrate and Fit Results of Sample 1[a]

structural feature	crystallographic average value[b] (range)	*N*	distance/angle	bond/angle variance	β
Cu−O1	1.955 (1.95−1.96)	2	1.95	0.004	
Cu−N	2.00 (1.98−2.02)	2	1.99	0.004	
Cu−C1	2.855 (2.83−2.88)	2	2.84	0.020	
Cu−C2	2.76 (2.75−2.77)	2	2.79	0.003	
C2−O2	1.235 (1.23−1.24)	2	1.24	0.006	
N−Cu−O1	176.0 (175−178)	2	179	36	
Cu−C2−O2	163.1 (162.0−164.3)	2	168	36	
$Cu-O_{ax}$	2.40	2	2.40(0.06)	0.03(0.01)	1.2(0.6)
$Cu-O_s$		4(3)	3.3(0.2)	0.06(0.03)	1.1(0.4)

[a] Distances and angles are given in Å and degrees, respectively. Bond and angle variances are reported in $Å^2$ and deg^2, respectively. *N* represents the coordination number and β the skewness of the asymmetric peaks. For the parameters that have been varied during the minimization, the standard deviations are given in parentheses. [b] Reference 41.

estimated statistical errors associated with the 95% confidence interval have been obtained as described elsewhere.[34,51] The standard deviation values associated with the $Cu-O_s$ shell parameters are rather large. These relatively large errors arise because of the use of a single asymmetric shell accounting for both the solvent and the free ligand molecules. However, the inclusion of the solvent shell in the minimization procedure provides a significant improvement, as deduced from the statistical *F* test.[52]

The outstanding observation of this investigation concerns the CuL_2 coordination at the axial site. The present analysis has shown the existence of a strongly distorted octahedral shell around the Cu^{2+} ion with two oxygens at 2.40 ± 0.06 Å. This value coincides with the distance observed in the bis(glycinato)-copper(II) monohydrate crystal and is significantly longer than the $Cu-O_{ax}$ average distance of Cu^{2+} complexes in aqueous electrolyte solutions.[32,36,53] This finding suggests that in the case of the CuL_2 complex in aqueous solution the formation of a strong Cu^{2+}−water oxygen interaction at the axial site is hampered by the presence of the two glycine ligands in the equatorial plane.

Structure of the Mono(glycinato)copper(II) Complex. The formation of Cu(II)−glycinate complexes is a function of $-\log c_h$, and the concentration of the different species present in solution can be evaluated from their stability constants. The distribution of the complexes reveals that CuL cannot be obtained as the only species in solution. To estimate the structural parameters of the mono(glycinato)Cu(II) complex, samples 2 and 3 have been investigated. According to the stability constants, solution 2 contains comparable amounts of CuL and CuL_2 complexes (39% and 60%, respectively) and negligible amounts of the other species. Sample 3 contains the CuL complex as predominant species (54.6%), but small amounts of CuHL and $Cu[(OH_2)_6]^{2+}$ complexes are present in solution together with CuL_2 (33.0%). During the EXAFS refinement the coordination numbers have been fixed according to the concentration ratios of the complexes. Starting structural parameters for the CuL_2 species have been derived from the analysis of sample 1. For the CuL complex the glycine ligand forms a five-member chelate with the amino and carboxylate groups bound to the Cu^{2+} ion in the equatorial plane. To retain the octahedral coordination, two additional water oxygens are placed in the equatorial positions at a distance of 1.96 Å. The Cu^{2+} coordination is completed by two additional oxygens at 2.4 Å.

The Cu(II)−ligand and $Cu-O_{eq}$ coordination numbers (1.6 and 0.8, respectively), determined from the concentration species, have been kept fixed during the minimization. The intensities of the Cu−C1, Cu−C2, and Cu−C2−O2 signals allow the CuL_2 complex to be distinguished from the CuL complex. Slight errors of the species concentrations do not significantly affect the amplitudes of these signals. In fact, a variation of +5% and −5% of the CuL and CuL_2 concentrations, respectively, induces a decrease of only 3% in the three contributions mentioned above.

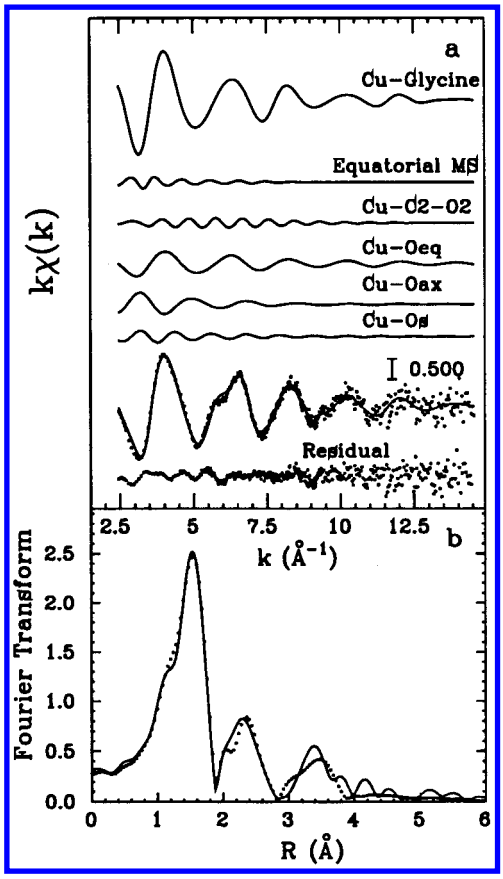

Figure 4. Comparison of the theoretical (−) and experimental (···) signals of the *k*-weighted EXAFS data and FT of sample 2; (a) from top to bottom, total Cu−glycine SS, equatorial MS, Cu−C2−O2, $Cu-O_{eq}$, $Cu-O_{ax}$, and $Cu-O_s$ calculated signals, their sum compared with the experimental spectrum, and the residual; (b) nonphase-shift-corrected FT of the experimental data and of the total theoretical signal.

The EXAFS minimization has been carried out by treating the carboxyl and the equatorial water oxygens as separate SS signals, since they were expected to have different DW factors. In Figures 4a and 5a the best-fit analyses for the EXAFS spectra of samples 2 and 3 are presented. The corresponding FTs are shown in Figures 4b and 5b, respectively. The overall agreement between the experimental and theoretical signals is satisfactory. Besides the SS and MS signals previously

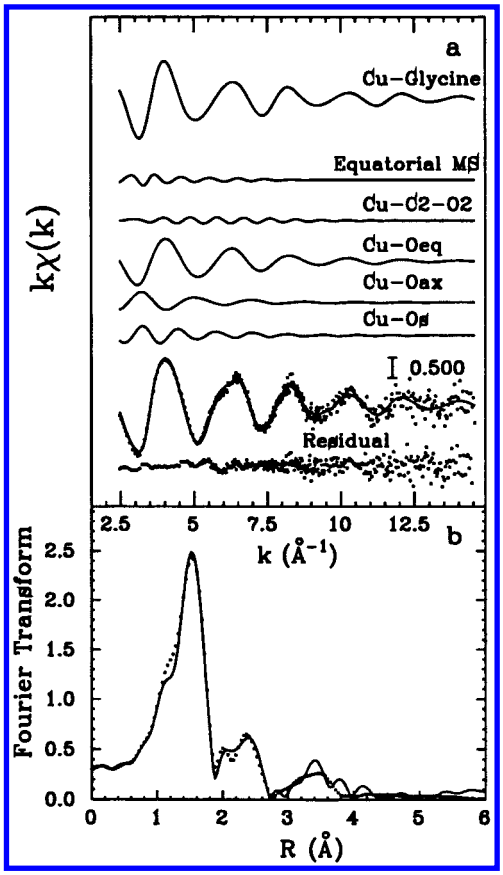

Figure 5. Comparison of the theoretical (−) and experimental (···) signals of the *k*-weighted EXAFS data and FT of sample 3: (a) from top to bottom, total Cu−glycine SS, equatorial MS, Cu−C2−O2, Cu−O_{eq}, Cu−O_{ax}, and Cu−O_s calculated signals, their sum compared with the experimental spectrum, and the residual; (b) nonphase-shift-corrected FT of the experimental data and of the total theoretical signal.

described for sample 1, an additional contribution (C−O_{eq}) due to the Cu−water oxygen interaction at the equatorial sites is reported. The comparison of the relative strengths of the individual components in the EXAFS spectra of samples 1−3 is informative. As expected, the amplitudes of the SS Cu−glycine and of the MS Cu−C2−O2 contributions decrease with decreasing CuL_2 concentration, while the amplitude of the Cu−O_{eq} signal shows an opposite trend. This behavior is reflected in the magnitude of the second peak of the FTs, which decreases going from sample 1 to sample 3. Note that this peak is mainly ascribable to the nonbonding Cu−C distances of the Cu−glycine ring. The amplitudes of the remaining EXAFS signals are practically the same for the three samples. The structural parameters obtained from the fitting procedures are summarized for samples 2 and 3 in Tables 1s and 2s, respectively, in the Supporting Information. The distances and angles obtained from the minimization are consistent with those of sample 1. The Cu−O_{eq} distance of 1.96 Å coincides with the value previously determined for hexaaquocopper(II) complexes.[32,36,53]

One point needs to be stressed. Sample 3 contains a detectable amount of the CuHL (9.3%) and $[Cu(OH_2)_6]^{2+}$ (3.1%) complexes. In all likelihood, at low pH values the amino group is protonated and the carboxyl oxygen atom is coordinated to the Cu^{2+} ion. As a consequence, the monodentate ligand has a large conformational flexibility and gives rise only to a Cu−O_{eq} SS signal. Therefore, the coordination of the Cu^{2+} ion in the CuHL and $[Cu(OH_2)_6]^{2+}$ complexes is similar and the EXAFS technique does not allow the presence of CuHL species to be detected.

From these results it is clear that the mono(glycinato)copper(II) also has a distorted octahedral structure with the axial sites occupied by two water molecules at 2.40 Å. This finding indicates that the axial bonds within Cu(II) are lengthened upon formation of the mono(glycinato) complex and that the Cu(II)−water interaction at the axial site is weakened. It should be noted that the axial Cu−O length for the hexaaquocopper(II) species is shorter (2.27 Å) than that found in the CuL_2 and CuL complexes (2.43 Å). Fits with shorter Cu−O axial bond lengths were attempted, but independently of the initially assumed values, the refined distances converged to 2.43 Å.

The structure of mono(glycinato)Cu(II) complexes in aqueous solution was previously investigated by Ozutsumi et al. using XRD[22] and EXAFS spectroscopy.[25] The XRD study has been performed on a 1.2 M Cu(II) solution, assuming a 40:60 concentration ratio of the hexaaquocopper(II) to the mono(glycinato)copper(II) complexes. From this investigation Ozutsumi et al.[22] concluded that the CuL complex has a distorted octahedral geometry with one glycinate ion and two water molecules in the equatorial plane and two water molecules axially coordinated. The axial Cu−O bond length was found to be 2.27 Å. This result conflicts with the present study. To estimate the XRD structural parameters for the mono(glycinato)copper(II) complex, the theoretical peaks due to the intramolecular interactions of $[Cu(OH_2)_6]^{2+}$ and the O···O interactions in the bulk water had to be subtracted. The coordination geometry of the $[Cu(OH_2)_6]^{2+}$ ion was quoted from the work of Ohtaki and Maeda,[54] and it was assumed to be a Jahn−Teller distorted octahedron with four oxygens at 1.96 Å and two oxygens at 2.43 Å. The structure of the Cu^{2+}−water complex in aqueous solutions has been extensively investigated in the past 20 years by X-ray and neutron diffraction analyses and X-ray absorption spectroscopy. All these studies concluded that the hydration shell of Cu^{2+} has an elongated octahedral structure, with the level of distortion depending upon the experimental technique used in the determination. In particular, the Cu−O_{ax} distance was determined to be in the range 2.12−2.60 Å (see Table 1A in ref 53). Nevertheless, most of the XRD and EXAFS measurements indicate a Cu−O_{ax} distance of ∼2.3 Å, which is shorter than the one used by Ozutsumi et al. in the course of the XRD data analysis.[22] As a consequence, it is feasible that the two Cu−O_{ax} distances at 2.27 and 2.43 Å, attributed to the $[Cu(gly)(OH_2)_4]^+$ and to the $[Cu(OH_2)_6]^{2+}$ complexes, respectively, have been mistaken for one another.

The structure of the mono(glycinato)copper(II) complex in aqueous solution has been studied by Ozutsumi et al. also using the EXAFS technique.[25] The species distribution of the solution used for the EXAFS analysis was evaluated on the basis of the molar absorption coefficients of the individual copper(II) glycinato complexes. Structural results were obtained for a solution of 0.7 M in Cu(II) containing three species, namely, $[Cu(OH_2)_6]^{2+}$ (40%), CuL (52%), and CuL_2 (8%). Both equatorial and axial distances determined for the CuL complex were pratically the same as those obtained from the previous XRD investigation.[22] It is interesting to note that this EXAFS data analysis, unlike the former XRD study, has been performed assuming a Cu−O_{ax} distance of 2.27 Å for the $[Cu(OH_2)_6]^{2+}$ complex. Moreover, the EXAFS data analysis has been carried out on Fourier filtered data over a short *k* range ($4.0 < k < 12.5$ Å^{-1}) and by application of the plane-wave formalism.

Structure of the Tris(glycinato)Copper(II) Complex. To our knowledge, the crystal structure of the tris(glycinato)copper(II) complex is unknown. Electromotive-force measurements show that at high pH and C_L values, the copper(II) ion

coordinates a third glycinato ligand, but from this technique, it is not possible to assess whether the third glycine acts as a mono- or bidentate ligand with respect to the Cu^{2+} ion.

The structure of the tris(glycinato)copper(II) complex in solution was previously studied by XRD.[22] Owing to the small stability constant of this complex, the structural investigation was carried out on a 0.58 M Cu(II) solution containing a large excess of sodium and glycinate ions (glycinate/copper(II) concentration ratio of 13.7). The XRD data were explained by assuming a regular octahedral structure of the CuL_3 complex having the same Cu−O and Cu−N bond distances of 2.02 Å and the third glycinate acting as a bidentate ligand.

In the present study the EXAFS data analysis of sample 4 (93.4% and 6.6% of CuL_3 and CuL_2, respectively) has been carried out assuming different models for the CuL_3 complex. During the fitting procedure the coordination numbers have been fixed according to the concentration ratios of the complexes. Structural parameters for the CuL_2 species have been derived from the previous analyses.

First, fits of the EXAFS experimental data were performed using a regular octahedral model for the CuL_3 complex, with three glycine molecules having the same Cu−O and Cu−N distances. Comparison of the amplitude of the EXAFS experimental and calculated spectra shows that the calculated signal is overestimated. In particular, the magnitude of the second and third peaks of the calculated FT is much too large compared with the experimental results. This result suggests that the third ligand provides a weaker contribution to the EXAFS signal and has a different coordination with respect to the glycine molecules in the equatorial positions. Moreover, from the CuL, CuL_2, and CuL_3 stability constant values, it appears that the $\log \beta_{1,0,3} - \log \beta_{1,0,2}$ difference (1.6) is smaller than $\log \beta_{1,0,2} - \log \beta_{1,0,1}$ (6.9). This finding confirms that the third ligand is weakly bound to the Cu^{2+} ion and that the possibility of a bidentate coordinating behavior with respect to the Cu^{2+} ion can be discounted.

Second, a CuL_3 model with two glycinato residues placed in the equatorial plane and a third one coordinated to the Cu^{2+} ion in the axial position through its nitrogen atom (N_{ax}) has been used in the EXAFS data analysis. The rationale for choosing a Cu−N coordination comes from the well-known preference of the Cu−amino coordination at increasing pH values. The second axial position is occupied by a water oxygen atom. The Cu−L, Cu−N_{ax}, and Cu−O_{ax} coordination numbers (2.00, 0.93, and 1.07, respectively) have been kept fixed during the minimization. This allowed the CuL_3 and CuL_2 concentrations to be preserved. A second hydration shell that roughly accounts for both the third ligand chain and the water molecules interacting with the complex has been included also. The Cu−L parameters have been moved in the same intervals used in the previous analyses, whereas the Cu−O_{ax}, Cu−N_{ax}, and Cu−O_s structural parameters and the second hydration-shell coordination number have been varied in a wide range during the minimization.

The best-fit analysis of the EXAFS spectrum of sample 4 and its FT are shown in parts a and b of Figure 6, respectively. The good agreement between the experimental and calculated spectra shows the substantial correctness of this model. The theoretical signals shown in Figure 6a are the same as previously described for sample 1, with the exception of the axial signal, which contains both the water Cu−O_{ax} and the third glycine Cu−N_{ax} contributions. The parameters obtained after minimization are listed in Table 2. The Cu−O_{ax} distance is consistent with the values found for the other samples analyzed in this paper. The Cu^{2+} coordination with the third glycine cannot be completely defined. The conformational flexibility of the monodentate coordinating ligand does not allow the structural parameters of all the atoms of the glycine chain to be determined. The Cu−N_{ax} bond length value (2.33 ± 0.05 Å) is larger than the typical Cu(II)−amino acid coordination distances (2.0 Å), showing a weaker link to the Cu^{2+} ion.

Attempts to individualize the Cu−C1 shell contribution have been unsuccessful. Minimization trials considering either a collinear Cu−N_{ax}−C1 geometry (Cu−C1 = 3.80 Å) or a Cu−N_{ax}−C1 angle around 110° (Cu−C1 = 3.16 Å) have been

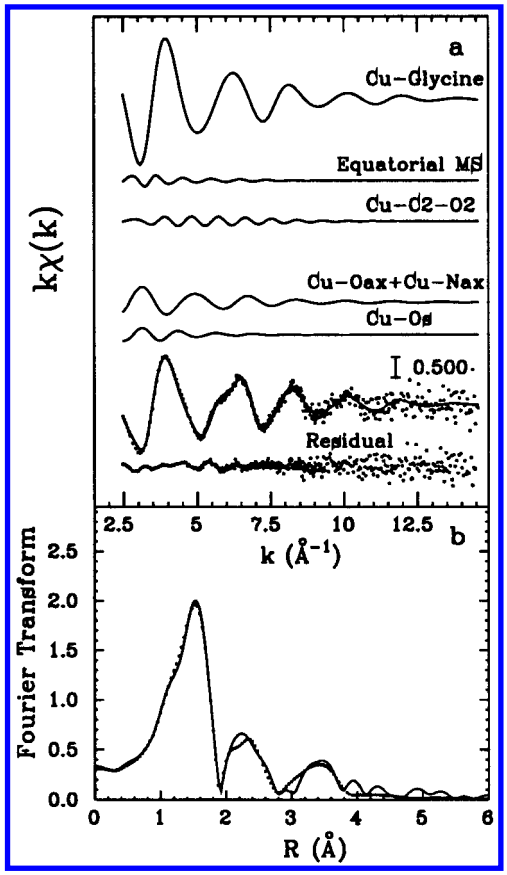

Figure 6. Comparison of the theoretical (−) and experimental (···) signals of the *k*-weighted EXAFS data and FT of sample 4: (a) from top to bottom, total Cu−glycine SS, equatorial MS, Cu−C2−O2, Cu−O_{ax} + Cu−N_{ax}, and Cu−O_s calculated signals, their sum compared with the experimental spectrum, and the residual; (b) nonphase-shift-corrected FT of the experimental data and of the total theoretical signal.

TABLE 2: Fit Results of Sample 4[a]

structural feature	*N*	distance/angle	bond/angle variance	β
Cu−O1	2	1.96	0.006	
Cu−N	2	2.02	0.007	
Cu−C1	2	2.89	0.020	
Cu−C2	2	2.79	0.010	
C2−O2	2	1.24	0.003	
N−Cu−O1 (O−Cu−O)	2	179	34	
Cu−C2−O2	2	168	40	
Cu−O_{ax}	1.07	2.41(0.06)	0.03(0.01)	1.6(0.9)
Cu−O_s	5(4)	3.40(0.08)	0.07(0.02)	0.9(0.7)
Cu−N_{ax}	0.93	2.33(0.05)	0.010(0.006)	

[a] Distances and angles are given in Å and degrees, respectively. Bond and angle variances are reported in $Å^2$ and deg^2, respectively. *N* represents the coordination number and β the skewness of the asymmetric peaks. For the parameters that have been varied during the minimization, the standard deviations are given in parentheses.

performed. In both cases, the Cu−C1 EXAFS signals were weak and the statistical *F* test showed that the inclusion of these contributions in the minimization procedure was not significant. In contrast, although the solvent shell has a coordination number with a large standard deviation, the statistical significance test was positive.

Conclusions

A structural investigation of the Cu(II)−glycine complexes in aqueous solution has been carried out by X-ray absorption spectroscopy. The presence of the $[CuL(OH_2)_4]^+$, $[CuL_2(OH_2)_2]$, and $[CuL_3(OH_2)]^-$ species and their respective concentrations have been determined on the basis of the stability constants previously obtained from emf measurements.

We have shown that a reliable data analysis procedure for these systems has to include multiple-scattering signals, mainly related to the equatorial coordination, and the presence of the 1s3p double-electron excitation channel. Use of the EXAFS technique in fluorescence mode allowed structural information to be obtained for dilute Cu(II) solutions (5 mM), which cannot be investigated by diffraction methods. The structure of the bis(glycinato)copper(II) complex, which has low solubility in water, has been determined for the first time in solution. It has been found to have a distorted octahedral geometry with two glycine molecules coordinating to the Cu^{2+} ion in the equatorial plane and two water molecules placed in the axial sites at 2.40 Å.

A detailed description and comparison of the structures of the mono- and tris(glycinato)copper(II) complexes have been made with reference to the previously reported structures obtained from XRD and EXAFS measurements. The former complex has an axially elongated octahedral structure with the glycine ligand and two water molecules placed in the equatorial plane and with the axial sites occupied by two additional water molecules at 2.44 Å. Also, for the latter complex a distorted octahedral structure has been obtained with the amino nitrogen of the third glycine coordinating to the Cu^{2+} ion at the axial site at a distance of 2.33 Å. This result conflicts with the regular octahedral geometry previously determined by XRD investigations.

The axial bond length found for the three complexes is significantly longer than the $Cu-O_{ax}$ average distance of Cu^{2+} complexes in aqueous electrolyte solutions. This finding indicates that the axial bonds are lengthened upon the formation of the Cu−glycine complexes and that the Cu(II)−water interaction at the axial site is weakened.

This study has allowed a precise description of the structure of the Cu−glycine complexes in addition to the highlighting of the advantages of using the EXAFS technique in the structural investigation of complexes in aqueous solution. These results represent a step forward in the EXAFS analysis of metal−amino acid complexes in solution and may stimulate further investigations of the structures of the tris(amino acidato)metal ion complexes that cannot be obtained in crystalline form.

Acknowledgment. The authors thank the European Union for support of the work at EMBL through the HCMP Access to Large Installation Project, Contract No. CHGE-CT93-0040. P. D'Angelo was supported by EU Contract No. ERBCHBGCT930485. This work was sponsored by the Italian CNR and by the Italian MURST.

Supporting Information Available: Experimental section on materials and electromotive-force measurements, and Tables 1s and 2s showing the fit results of samples 2 and 3 (3 pages). Ordering information is given on any current masthead page.

References and Notes

(1) Abbreviations: DW, Debye−Waller; emf, electromotive force; EXAFS, extended X-ray absorption fine structure; FT, Fourier transform; L, glycinate ligand $H_2N-CH_2-COO^-$; C_{Cu}, total Cu(II) concentration; C_H, analytical excess of hydrogen ions; CuL and CuLH are mono(glycinato)copper(II) complexes; CuL_2 and CuL_3 are bis- and tris(glycinato)copper(II) complexes, respectively (in this notation charges are omitted); MS, multiple scattering; SS, single scattering; XAS, X-ray absorption spectroscopy; XRD, X-ray diffraction.

(2) Sarkar, B. In *Metals Ions in Biological Systems*; Sigel, H., Sigel, A., Eds.; Marcel Dekker: New York, 1981; Vol. 12, pp 233−256.

(3) *Handbook on Metals in Clinical and Analitical Chemistry*; Seiler, H., Sigel, A., Sigel, H., Eds.; Marcel Dekker: New York, 1994.

(4) Harford, B.; Sarkar, B. In *Handbook of Metal−Ligand Interactions in Biological Fluids Bioinorganic Medicine*; Berthon, G., Ed.; Marcel Dekker: New York, 1996; Vol. 1, pp 62−70.

(5) Österberg, R. In *Handbook of Metal−Ligand Interactions in Biological Fluids Bioinorganic Medicine*; Berthon, G., Ed.; Marcel Dekker: New York, 1996; Vol. 1, pp 10−28.

(6) (a) Martell, A. E.; Sillén, L. G. In *Stability Constants*; The Chemical Society: London, 1964; Special Publication No. 17, pp 377−381. (b) Martell, A. E.; Sillén, L. G. In *Stability Constants*; The Chemical Society: London, 1971; Special Publication No. 25, pp 264−269.

(7) Perrin, D. D. *Stability Constants of Metal Ion Complexes, Part B: Organic Ligands*; IUPAC Chemical Data Series 22; Pergamon Press: New York, 1979; , pp 73−84.

(8) Pettit, L. D.; Powell, H. K. J. *IUPAC Stability Constants Database*; Academic Software: Otley, Yorkshire, 1993.

(9) Martell, A. E.; Smith, R. M. *Critical Stability Constants*; Plenum Press: New York, 1982; Vol. 5, pp 1−2.

(10) Kiss, T.; Sóvágó, I.; Gergely, A. *Pure Appl. Chem.* **1991**, *63*, 597−638.

(11) Yamauchi, O.; Odani, A. *Pure Appl. Chem.* **1996**, *68*, 469−496.

(12) Biedermann, G.; Sillén, L. G. *Ark. Kemi* **1953**, *5*, 425−440.

(13) Sarkar, B.; Kruck, T. P. A. In *Biochemistry of Copper*; Peisach, J., Aisen, P., Blumberg, W. E., Eds.; Academic Press: New York, 1966; pp 183−196.

(14) Pickart, L.; Freedman, J. H.; Loker, W. J.; Peisach, J.; Perkins, C. M.; Stenkamp, R. E.; Weinstein, B. *Nature* **1980**, *288*, 715−717.

(15) Laurie, S. H. In *Handbook of Metal−Ligand Interactions in Biological Fluids Bioinorganic Chemistry*; Berthon, G., Ed.; Marcel Dekker: New York, 1996; Vol. 1, pp 603−619.

(16) (a) Liang, Y.-C.; Olin, Å. *Acta Chem. Scand.* **1984**, *A38*, 247−252. (b) Al-Ami, N.; Olin, Å. *Chem. Scr.* **1983**, *22*, 105−107. (c) Al-Ami, N.; Olin, Å. *Chem. Scr.* **1984**, *23*, 161−164. (d) Al-Ami, N.; Olin, Å. *Chem. Scr.* **1984**, *23*, 165−169.

(17) Bottari, E.; Jasionowska, R.; Porto, R. *Ann. Chim. (Rome)* **1983**, *73*, 15−27.

(18) (a) Bottari, E.; Jasionowska, R. *Ann. Chim. (Rome)* **1978**, *68*, 517−524. (b) Bottari, E.; Festa, M. R.; Jasionowska, R. *Ann. Chim. (Rome)* **1987**, *77*, 837−851. (c) Bottari, E.; Festa, M. R.; Jasionowska, R. *Polyhedron* **1989**, *8*, 1019−1027. (d) Bottari, E.; Festa, M. R.; Jasionowska, R. *Chem. Scr.* **1989**, *29*, 85−89. (e) Bottari, E.; Festa, M. R.; Jasionowska, R. *J. Coord. Chem.* **1989**, *20*, 209−217. (f) Bottari, E.; Festa, M. R.; Jasionowska, R. *J. Coord. Chem.* **1990**, *21*, 215−224. (g) Bottari, E.; Festa, M. R. *J. Coord. Chem.* **1990**, *22*, 237−248.

(19) Freeman, H. C. *Adv. Protein Chem.* **1967**, *22*, 257−424.

(20) Laurie, S. H. In *Comprehensive Coordination Chemistry*; Wilkinson, G., Gillard, R. D., McCleverty, J. A., Eds.; Pergamon Press: Oxford, 1987; Vol. 2, pp 739−766.

(21) Ozutsumi, K.; Ohtaki, H. *Bull. Chem. Soc. Jpn.* **1983**, *56*, 3635−3641.

(22) Ozutsumi, K.; Ohtaki, H. *Bull. Chem. Soc. Jpn.* **1984**, *57*, 2605−2611.

(23) Ozutsumi, K.; Ohtaki, H. *Bull. Chem. Soc. Jpn.* **1985**, *58*, 1651−1657.

(24) Ozutsumi, K.; Yamaguchi, T.; Ohtaki, H.; Tohji, K.; Udagawa, Y. *Bull. Chem. Soc. Jpn.* **1985**, *58*, 2786−2792.

(25) Ozutsumi, K.; Miyata, Y.; Kawashima, T. *J. Inorg. Biochem.* **1991**, *44*, 97−108.

(26) Bottari, E. *Ann. Chim. (Rome)* **1976**, *66*, 139−154.

(27) The equilibria

$$q\mathrm{Cu} + p\mathrm{H} + r\mathrm{L} \overset{\beta_{qpr}}{\rightleftharpoons} \mathrm{Cu}_q\mathrm{H}_p\mathrm{L}_r$$

are described by the stability constants β_{qpr}, defined by the equation $c_{\mathrm{Cu}_q\mathrm{H}_p\mathrm{L}_r} = \beta_{qpr} c_{\mathrm{Cu}}{}^q c_{\mathrm{h}}{}^p c_{\mathrm{L}}{}^r$, where c_{Cu} and c_{L} are the concentrations of free Cu^{2+} and

glycinate ions, respectively. In this notation, charges are omitted. From the balance relative to C_H, taking into account the mass-action law, c_L can be calculated for each experimental point:

$$C_H = c_h + K_1 c_h c_L + 2K_1 K_2 c_h^2 c_L + \sum_q \sum_p \sum_r p\beta_{qpr} c_{Cu}^q c_h^p c_L^r$$

K_1 and K_2 are the protonation constants of glycinate. Their values were determined in 1.00 M $NaClO_4$ as ionic medium, by measuring the emf of a galvanic cell containing a hydrogen electrode, as a function of the hydrogen and glycine total concentrations (C_L). The protonation constant values obtained were $\log K_1 = 9.73 \pm 0.03$ and $\log(K_1K_2) = 12.22 \pm 0.04$.[26]

(28) Berecki-Biedermann, C. *Ark. Kemi* **1956**, *9*, 175−189.
(29) Bottari, E.; Siliberti, P. *Ann. Chim. (Rome)* **1976**, *66*, 629−644.
(30) Hermes, C.; Gilberg, E.; Koch, M. H. J. *Nucl. Instrum. Methods* **1984**, *A222*, 207−214.
(31) Pettifer, R. F.; Hermes, C. *J. Appl. Crystallogr.* **1985**, *18*, 404−412.
(32) D'Angelo, P.; Bottari, E.; Festa, M. R.; Nolting, H.-F.; Pavel, N. V. *J. Chem. Phys.* **1997**, *107*, 2807−2812.
(33) Filipponi, A.; Di Cicco, A.; Natoli, C. R. *Phys. Rev. B* **1995**, *52*, 15122−15134.
(34) Filipponi, A.; Di Cicco, A. *Phys. Rev. B* **1995**, *52*, 15135−15149.
(35) D'Angelo, P.; Di Nola, A.; Filipponi, A.; Pavel, N. V.; Roccatano, D. *J. Chem. Phys.* **1994**, *100*, 985−994.
(36) Filipponi, A.; D'Angelo, P.; Pavel, N. V.; Di Cicco, A. *Chem. Phys. Lett.* **1994**, *225*, 150−155.
(37) D'Angelo, P.; Di Nola, A.; Giglio, E.; Mangoni, M.; Pavel, N. V. *J. Phys. Chem.* **1995**, *99*, 5471−5480.
(38) D'Angelo, P.; Nolting, H.-F.; Pavel, N. V. *Phys. Rev. A.* **1996**, *53*, 798−805.
(39) D'Angelo, P.; Di Nola, A.; Mangoni, M.; Pavel, N. V. *J. Chem. Phys.* **1996**, *104*, 1779−1790.
(40) D'Angelo, P.; Pavel, N. V.; Roccatano, D.; Nolting, H.-F. *Phys. Rev. B* **1996**, *54*, 12129−12138.
(41) Freeman, H. C.; Snow, M. R. *Acta Crystallogr.* **1964**, *17*, 1463−1470.
(42) Hedin, L.; Lundqvist, B. I. *J. Phys. C* **1971**, *4*, 2064−2083.
(43) Di Cicco, A.; Sperandini, F. *Physica C* **1996**, *258*, 349−359.
(44) Stern, E. A. *Phys. Rev. B* **1993**, *48*, 9825−9827.
(45) (a) Shulman, R. G.; Yafet, T.; Eisenberger, P.; Blumberg, W. E. *Proc. Natl. Acad. Sci. U.S.A.* **1976**, *73*, 1384−1388. (b) Hahn, J. E.; Scott, R. A.; Hodgson, K. O.; Doniach, D.; Dejardins, S. E.; Solomon, E. I. *Chem. Phys. Lett.* **1982**, *88*, 595−598.
(46) (a) Smith, T. A.; Penner-Hahn, J. E.; Berding, M. A.; Doniach, S.; Hodgson, K. O. *J. Am. Chem. Soc.* **1985**, *107*, 5945−5955. (b) Kau, L.-S.; Spira-Solomon, D. J.; Penner-Hahn, J. E.; Hodgson, K. O.; Solomon, E. I. *J. Am. Chem. Soc.* **1987**, *109*, 6433−6442. (c) Shadle, S. E.; Penner-Hahn, J. E.; Schugar, H. J.; Hedman, B.; Hodgson, K. O.; Solomon, E. I. *J. Am. Chem. Soc.* **1993**, *115*, 767−776.
(47) Pickering, I. J.; George, G. N. *Inorg. Chem.* **1995**, *34*, 3142−3152.
(48) Zippel, F.; Ahlers, F.; Werner, R.; Haase, W.; Nolting, H.-F.; Krebs, B. *Inorg. Chem.* **1996**, *35*, 3409−3419.
(49) Boswell, J. S.; Reedy, B. J.; Kulathila, R.; Merkler, D.; Blackburn, N. J. *Biochemistry* **1996**, *35*, 12241−12250.
(50) Delf, B. W.; Gillard, R. D.; O'Brien, P. *J.C.S. Dalton* **1979**, 1301−1305.
(51) Filipponi, A. *J. Phys.: Condens. Matter* **1995**, *7*, 9343−9356.
(52) Bevington, P. R. *Data Reduction and Error Analysis for the Physical Sciences*; McGraw-Hill: New York, 1969.
(53) Okan, S. E.; Salmon, P. S. *Mol. Phys.* **1995**, *85*, 981−998.
(54) Ohtaki, H.; Maeda, M. *Bull. Chem. Soc. Jpn.* **1974**, *47*, 2197−2199.